2014 IEEE International Conference on Robotics & Automation (ICRA)
Hong Kong Convention and Exhibition Center
May 31 - June 7, 2014. Hong Kong, China

Mechanical Design and Implementation of a Soft Inflatable Robot Arm for Safe Human-Robot Interaction

Ronghuai Qi, Tin Lun Lam, and Yangsheng Xu

***Abstract*— In this paper, a novel soft inflatable arm is proposed for telepresence robots. It is capable of imitating human arms to realize remote interaction. The new proposed arm using a very common and low cost inflatable material, and it is very light, which weight is only about 50 grams, but can well realize agile movement by driving three tiny cables installed in shoulder joint and elbow joint, respectively. Meanwhile, the proposed cable driven mechanism also allows connecting numbers of joints easily. The soft inflatable can work just by pumping air with very low pressure (7.32 ± 3.45 kPa), and allows human directly and safely contact without any external sensors.**

Moreover, to solve the challenge problems of soft joint deformation, the kinematic modeling of the joint with deformation compensation is also developed. Experimental results show that the soft inflatable arm can agilely move for remote interaction. The workspace and velocity are also close to an adult's arm movement space and normal motion speed.

I. INTRODUCTION

A robot arm that is to interact with humans has a single design consideration at a premium – safety [1-4]. Some new approaches focus on solving human safe problems [3-7], such as using inflatable materials or other plastic materials [8-15]. And these inflatable robots are new research topics in recent years [9-11], as they have many advantages and desirable properties. For instance, they are composed of fabric and basic pneumatic parts (eg. an air supply, valves, and tubing). The manufacturing cost can be very low. They also possess high strength-to-weight ratios owing to the strength of pneumatics and the mostly air-and-fabric structural members. In addition, they are naturally compliant, which makes them human-safe[6-9]. But, there also remains some challenge problems, such as deformation and kinematics of the soft joint [6,14-15].

Some researchers did investigations on them. Siddharth Sanan [14-15] developed a soft robot arm, which weights up to 500 grams and has 2DOF, and can move only in a plane by driving two cables. Otherlab [16] designed another inflatable walking elephant called Ant-Roach. This robot used textile-based, inflatable actuators that contract upon inflation into specially-designed shapes to effect motion. Since this robot is built out of fabric-and-air structural members and powered via pneumatics or hydraulics, it exhibited large strength-to-weight ratios. Otherlab [16] seems focus on payload target, since Ant-Roach is less than 32 kilograms but can probably support up to about 454kg. In the same year, Otherlab also developed another inflatable robot arm [16], which is a lightweight, low-cost inflatable robotic arm, and it is extremely powerful. And the arm weighs is about 2kg and is still able to lift several hundred pounds (eg. a person) with 400 kPa. Saul [17] designed another inflatable walking elephant, he involved to use compressed air to drive mechanical motion. However, the structures of these robots or arms are much heavier, need higher pressure or can only move in a plane. It shows that the minimum weight is 500 grams, and 400 kPa in pressure.

Fig. 1. The telepresense robot

In this paper, we present a novel structure of soft inflatable arm. To evaluate the performances and demonstrate the application of the novel inflatable arm, two arms are installed on a telepresense robot, which are shown in Fig. 1. The proposed arm is much lighter and needs lower pressure, which weight is only about 50 grams, and 7.32 ± 3.45 kPa in pressure. Meanwhile, we developed new drive structures by six micro cables hidden in the robot to well realize agile movement, and the proposed cable driven mechanism also allows connecting numbers of joints easily. It is also capable of imitating human arms to realize remote interaction. Most of the cables are wired inside the arm and make results in a

This work is supported in part by the Smart China Research Project (HK201305001).

Ronghuai Qi and Tin Lun Lam are with the Intelligent Robotics Research Centre, Smart China Research, Smart China Holdings Limited, Shatin, N.T., Hong Kong {ronghuai.qi, tinlun.lam}@smartchinaholdings.com

Yangsheng Xu is with the Dept. of Mechanical and Automation Engineering, The Chinese University of Hong Kong, Shatin, N.T., Hong Kong ysxu@mae.cuhk.edu.hk

tidy appearance. Also, it is safer and allows human directly contact without any external sensors.

To solve the challenge problem of soft joint deformable problems as mentioned above, we develop a new joint model, joint compressed length and joint kinematics algorithms to accomplish the target. Numerous experiments have been conducted and the results also show that the soft inflatable arms not only can agilely move, but also make more complex motions, like dancing. The workspace and velocity are close to an adult's arm movement space and normal motion speed.

In Section II, we introduce the mechanical design and implantation of the inflatable arm. In Section III, a new joint model and algorithms are developed based on the designed inflatable arm. In Section IV, the experiments and results are proposed. In Section V, the contributions of the current work and future work are concluded.

II. MECHANICAL DESIGN AND IMPLEMENTATION

The proposed mechanical model of the soft inflatable arm is shown in Fig. 2. The arm structure is based on Thermoplastic Polyurethane (TPU), which is a very common, low cost, and environmental friendly inflatable material. The length of upper arm and lower arm are 190mm and 190mm. The thickness of the soft inflatable is 0.18mm, and the weight is only about 50 grams. The enlarged structures of the shoulder joint and elbow are shown in Fig. 3 and Fig. 4, respectively. The arms can be driven by three cables (diameter is 0.3mm) installed in the shoulder joint and elbow joint, respectively. Each cable in the arm pass though shoulder driven tubes, and elbow driven tubes, fixed on the shoulder joint and elbow joint by a pair of micro nozzle unit, which contains a micro steel nozzle, a nut and a plastic tab. And these tubes are used to avoid air leakage and protect cables. Shoulder driven tubes and elbow driven tubes are connected to external driven tubes. The external driven tubes are connected to driven actuators. The arm can be moved by pulling six cables by driven actuators. Shoulder connector is used to connect the arm to the robot body, with its diameter 57mm, and thickness 9mm. The gas tubes are used to inflate and deflate air. In addition, rubber seal ring is used to avoid leak gas, which thickness equals 1mm.

The shapes of shoulder joint and elbow joint are cambers (shown in Fig. 3 and Fig. 4), which are used for bending the joints easily. The middle section diameter is 40mm, and both ends diameters and are 70mm (refer to human arms), respectively. Analysis of selecting these parameters will be discussed in section III.

Moreover, the nozzle units and cables can installed on the soft arm by the following steps: First, the plastic tabs (the same material with the soft arm) are welded on the soft inflatable arm by a common high frequency welding machine(high frequency plastic welding) [18]. Second, the micro steel nozzle and tubes are fixed on the arm by their corresponding nuts. Third, one ends of the cables are tied on the plastic tabs, and the other ends pass though the nuts,

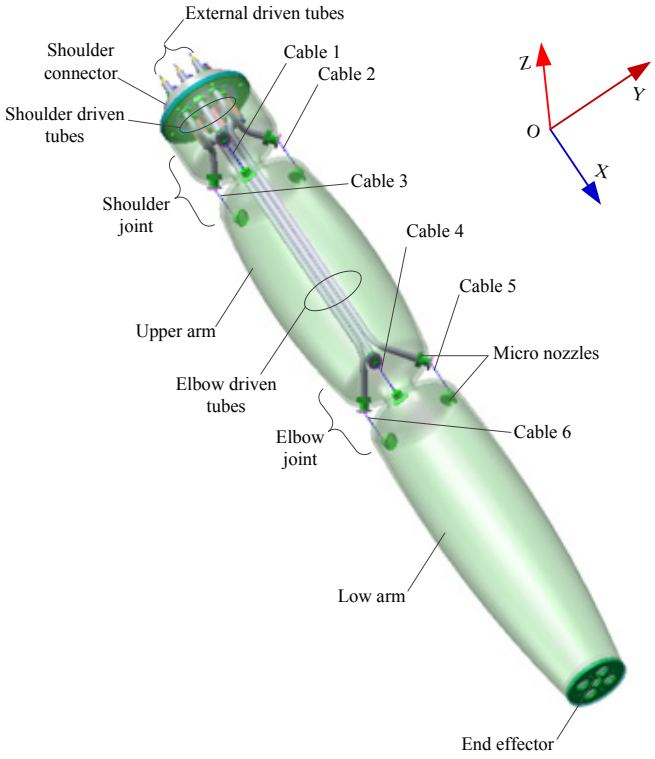

Fig. 2. The mechanical model of the right soft inflatable arm

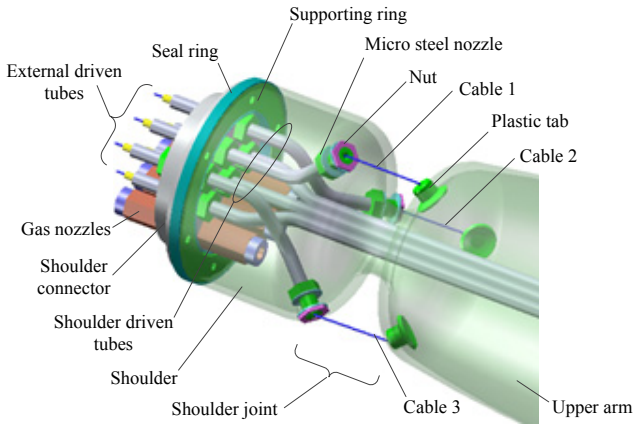

Fig. 3. Enlarged structure of the shoulder joint

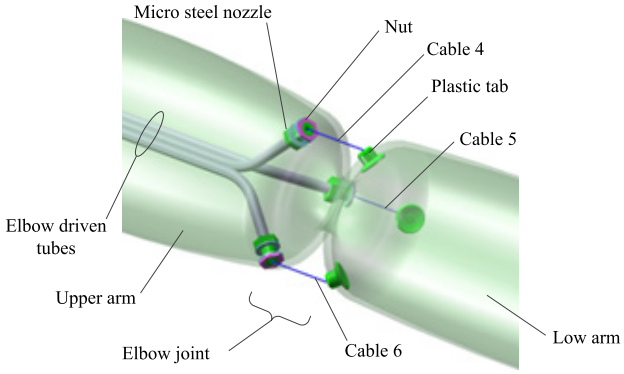

Fig. 4. Enlarged structure of the below joint

the micro steel nozzles, the tubes, and finally are tied on the driven actuators.

Fig. 5 shows the structure of cable driven unit, which includes four parts. The tube has two layers, the outside is a plastic tube, which inside diameter is 2mm, and outside diameter is 3mm. The other tube is a steel spring tube, which outside diameter is 1.6mm, and inside is 1mm. The steel tube is used to protect and support the plastic tube and cable. The inflatable arm has relative low rigid, so the cable should be careful selected to avoid bigger friction to make the inside cables cannot move. Experimental results show that, the diameter of steel cable equals 0.3mm is better. The Micro nozzle is contained by barbs and screw bolt. Barbs are used to connect the plastic tube firmly, and screw bolt is used to connect the soft arm with the actuator driven unit. In addition, the driven tube can be very long, so driven actuators can be installed remotely, such as the bottom of the robot body as shown in Fig. 1.

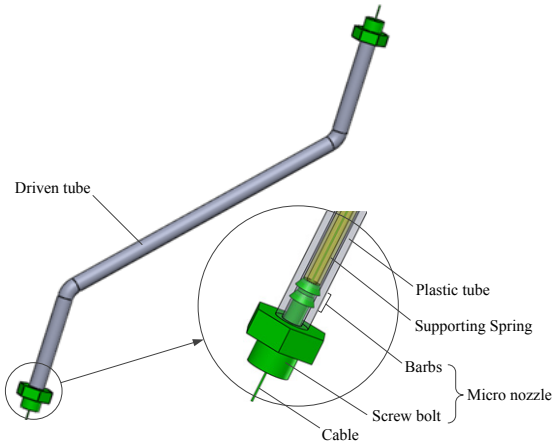

Fig. 5. Structure of cable driven unit

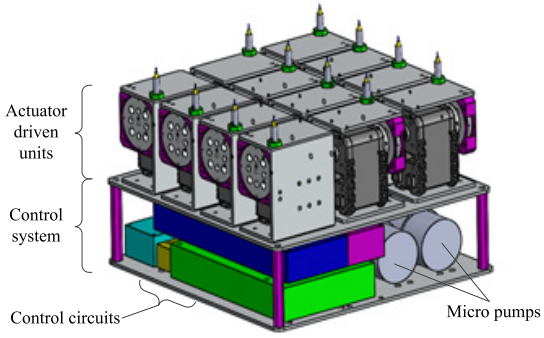

Fig. 6. The control system

Fig. 6 shows the micro control system, with its length, wideness, and height equals 180mm, 180mm, and 118mm, respectively. And the weight is 2.25kg, which is small and light, and it can be easily fixed on the bottom of the robot. The control system mainly contains a MCU module, twelve micro servo actuators (DYNAMIXEL AX-12A) based cable driven units, pressure sensors, mini pumps, and a blue teeth module. The control system is based on STM32F4 controller. The blue teeth module is easy and good interface to realize wireless motion control. These twelve micro servo actuators based cable driven units are used to control two soft inflatable arms to move. Six driven units are used to control left arm and the others are used to control right arm.

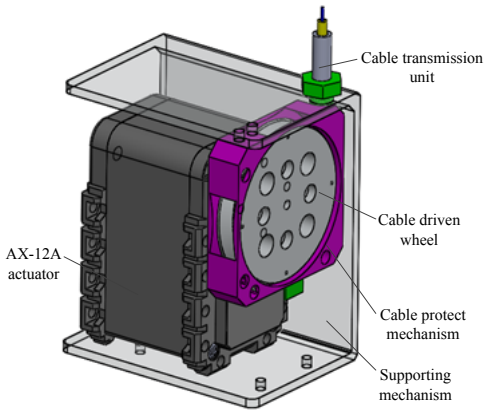

Fig. 7. Single actuator driven unit

Fig. 8. The actual soft inflatable arm

Fig. 7 shows a single cable drive unit. The AX-12A actuator and cable protect mechanism are fixed on supporting mechanism, and the former is used to drive a cable turning around cable drive wheel, and the latter is used to avoid the cable drop out from the wheel. Since the cable is only 0.3mm, actually cable is very easily drop out from the wheel without this protecting mechanism. Numerous experiments show that this protect mechanics is effective, and almost no cables drop out.

By implementing the above designs and approaches, the actual soft inflatable arm is accomplished, which is shown in Fig. 8. After pumping air into the robot arm with 7.32 ± 3.45 kPa in pressure, the arm can be moved by pulling three tiny cables installed in shoulder joint and elbow joint, respectively. In addition, the arm merits of this novel soft inflatable arm is that, it combines the skin and framework as a whole, and very light, easy and low cost for fabrication. Meanwhile, most of the cables are wired inside the arm and make results in a tidy appearance.

III. JOINT MODELING

As we mentioned above, the shapes of shoulder joint and elbow joint are cambers (shown in Fig. 3 and Fig. 4), which

are used for bending the joints easily. Fig. 9 shows the cross section and front view of the joint. And the following assumptions are made for better analyzing. The middle section diameter d equals 40mm, and both ends diameters D_a and D_b equal 70mm. The diameters D_a and D_b is selected main refer to a normal human arm. When diameters D_a and D_b are fixed, if diameter d is larger, it is more difficult to rotate the soft inflatable joint, but the stiffness of the joint becomes worse, and vice versa. Numerous experiments have been conducted and the results show that when diameter d equals 40mm is an optimal solution to balance bending joint easily and joint rigidity.

Moreover, three points (P_{a1}, P_{a2}, P_{a3}), and (P_{b1}, P_{b2}, P_{b3}) are attached to the fixed base (plane A), and moving platform (plane B), respectively. Point P_0 is located at the center of joint. The connections from point P_{a1} to P_{b1}, P_{a2} to P_{b2}, and P_{a3} to P_{b3} are corresponding to cable 1, cable 2 and cable 3, or cable 4, cable 5 and cable 6, respectively. A cross-section C plane crosses point P_0, and moves with moving platform (plane B). And three cables are located as α_1, α_2, and α_3 equal $\frac{2\pi}{3}$, respectively. Let $\triangle \mathrm{P_{a1}P_0P_{b1}}$, $\triangle \mathrm{P_{a2}P_0P_{b2}}$ and $\triangle \mathrm{P_{a3}P_0P_{b3}}$ are in plane H_1, plane H_2 and plane H_3, respectively.

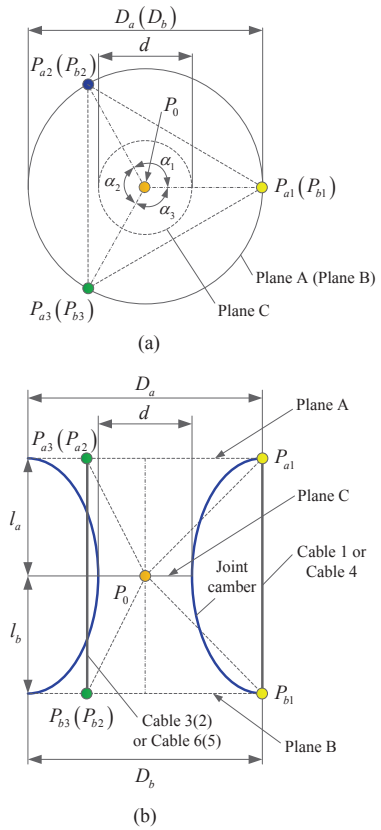

Fig. 9. Cross section and front view of joint

A new single joint driven model is proposed based on the above new soft inflatable arm is shown in Fig. 10, and the model is in plane H_i (plane H_1, plane H_2, or plane H_3), which is correspond to the cable. And θ is joint angle, L is cable length of the joint, h_a equals $D_a/2$, h_b equals $D_b/2$. In addition, we discovered that one of the challenge issues is when the arm was bent, the length of l_a and l_b is not a constant. So we assume Δl is the joint compressed length of l_a or l_b (experimental results show that the joint compressed length of l_a and l_b are general equal, so Δl is the assumed common compressed length). φ is the actuator rotation angle, with its initial angle equals zero. r is the drive wheel radium. This cable joint model is available to all twelve cables drive to realize arms moving in joint workspace.

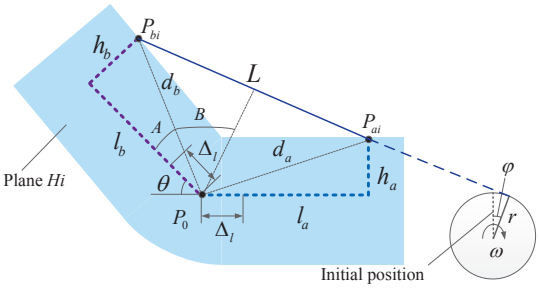

Fig. 10. Single cable driven model

A. Joint compressed length

As we mentioned above, when the arm is bent, the l_a or l_b are not constant, but follows a nonlinear, and Δl is assumed to elevate the variables.

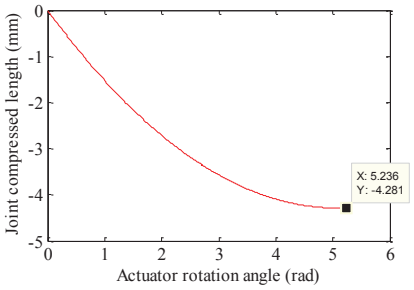

Fig. 11. Relationship between joint compressed length Δl and actuator rotation angle φ

We proposed a statistical method by bending the joint, gathering the length of l_a and l_b, and fitting the gathers values to find Δl. The results are shown in Fig. 11, where horizontal axis shows the value of Δl, and the vertical axis shows the actuator rotation angle φ, which follows the Eq. as,

$$\Delta l = 0.16663525\varphi^2 - 1.69013382\varphi \qquad (1)$$

where $\varphi \in [0, \frac{5\pi}{3}]$. And $[0, \frac{5\pi}{3}]$ equals the rotation region of servo actuators (DYNAMIXEL AX-12A). Of course, it can be apply to other actuators with larger region .

B. Joint kinematics

The joint kinematics model is shown in Fig.10. The target is to compute the equation between actuator rotation φ and the joint angle θ, as $\theta \rightarrow \varphi$. As the algorithm is available to each cable, so we take the cable in Fig. 10 as an instance to analyze.

As mentioned the different sizes of the arm above, let $l_a = l_b$=$l, h_a = h_b = h$, and $d_a = d_b = d$. l_{a0} and l_{b0} equal l_a and l_b, respectively, when φ equals zero. And $l_{a0} = l_{b0}$. The following Eq. can be descried as,

$$\theta+2\mathrm{A}+2\mathrm{B}=\pi \tag{2}$$

$$A = a\tan(\frac{h}{l}) \tag{3}$$

$$B = \frac{\pi}{2} - A - \frac{\theta}{2} \tag{4}$$

$$d = \sqrt{l^2 + h^2} \tag{5}$$

$$\frac{L}{2} = d_1 \sin B = \sqrt{l^2 + h^2}\sin B \tag{6}$$

$$L = 2\sqrt{l^2 + h^2}\cos(atan(\frac{h}{l}) + \frac{\theta}{2}) \tag{7}$$

$$\Delta L = L_0 + L = 2l_0 - L \tag{8}$$

where $L_0 = 2l_0$, $l = \Delta l + l_0$, $l_0 = l_{a0} = l_{b0}$. L_0 is a corresponding length of the cable. More Eq. can be calculated as,

$$L = 2\sqrt{(\Delta l + l_0)^2 + h^2}\cos(atan(\frac{h}{\Delta l + l_0}) + \frac{\theta}{2}) \tag{9}$$

$$\varphi r = 2l_0 - 2\sqrt{(\Delta l + l_0)^2 + h^2}\cos(atan(\tfrac{h}{\Delta l + l_0}) + \tfrac{\theta}{2}) \tag{10}$$

Simple Eq. (10) as,

$$\frac{\varphi r}{2} = -\Delta l\cos(\frac{\theta}{2}) + l_0 - l_0\cos(\frac{\theta}{2}) + h\sin(\frac{\theta}{2}) \tag{11}$$

In addition, from Eq. (1), let $C = 0.16663525$, $D = -1.69013382$. Then

$$\Delta l = C\varphi^2 + D\varphi \tag{12}$$

and then,

$$\tfrac{\varphi r}{2} = -(C\varphi^2 + D\varphi)\cos(\tfrac{\theta}{2}) + l_0 - l_0\cos(\tfrac{\theta}{2}) + h\sin(\tfrac{\theta}{2}) \tag{13}$$

Simple Eq.(13), then,

$$0 = -C\cos(\tfrac{\theta}{2})\varphi^2 + (-D\cos(\tfrac{\theta}{2}) - \tfrac{r}{2})\varphi + (l_0 - l_0\cos(\tfrac{\theta}{2}) + h\sin(\tfrac{\theta}{2})) \tag{14}$$

Let

$$\begin{cases} a = -C\cos(\frac{\theta}{2}) \\ b = -D\cos(\frac{\theta}{2}) - \frac{r}{2} \\ c = l_0 - l_0\cos(\frac{\theta}{2}) + h\sin(\frac{\theta}{2}) \end{cases} \tag{15}$$

then,

$$a\varphi^2 + b\varphi + c = 0 \tag{16}$$

The solutions of Eq. (16) can be described as,

$$\varphi = \frac{-b \pm \sqrt{b^2 - 4ac}}{2a} \qquad (a \neq 0) \tag{17}$$

As we defined the region of joint rotation angle as $\theta \in [0, \pi)$, then $\frac{\theta}{2} \in [0, \frac{\pi}{2})$, then $\cos\frac{\theta}{2} \in (0, 1]$, so $a \neq 0$.

Let Δ=$b^2 - 4ac$, and the result shows that $\Delta > 0$. As $\varphi \geq 0$, so the actuator rotation angle can be calculated as,

$$\varphi = \frac{-b - \sqrt{b^2 - 4ac}}{2a} \tag{18}$$

Moreover, others very useful equations can also be calculated as,

$$L = 2l_0 + r\varphi \tag{19}$$

$$l = C\varphi^2 + D\varphi + l_0 \tag{20}$$

Eq. (19) and Eq. (20) are the forward kinematics of the soft inflatable joint. The above equations are well developed to control each cable to drive the soft inflatable arm to move in joint coordinate system.

IV. EXPERIMENTAL RESULTS

The main target of the arms is to imitate human arms to realize remote interaction, like wave hand, shake hand, etc. To verify the agility of movement of the arm, we symmetrically install two arms on a telepresense robot, as the left and right arm for the robot, which shows in Fig.1. Of course, they can easily wear arm sleeves to harmonize with the body. Some examples the movement of the robot are developed to shows the useful and agile. Fig. 12 shows the robot is waving hand to say hello to somebody else. Fig. 13 shows the robot is shaking hand. In addition, it also can make more complex motions, like dancing, which are shown in Fig. 14 and Fig. 15, respectively.

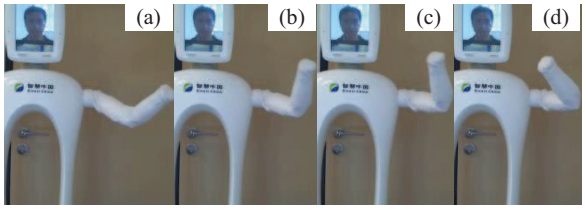

Fig. 12. The robot is waving hand

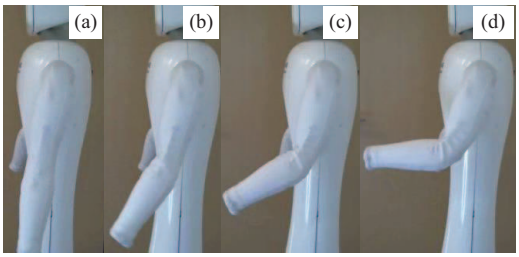

Fig. 13. The robot is shaking hand

As the above examples show, the soft inflatable arm with has capitals of agile movement. Numerous experimental results show that the end effector workspace in coordinate systems (the base system is built on shoulder joint as shown in Fig. 2) follows $x \in [0, 380]$, $y \in [0, 370]$ and $z \in [0, 360]$. The maximum velocity is about 250mm/s, which are close to an adult's arm movement space and normal motion speed[19-24].

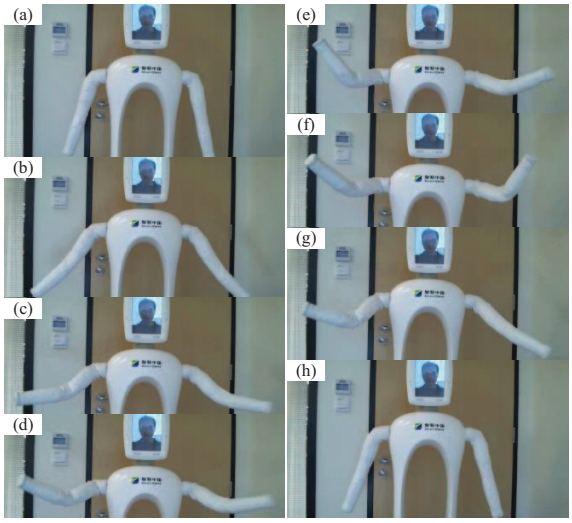

Fig. 14. The robot is dancing with one style

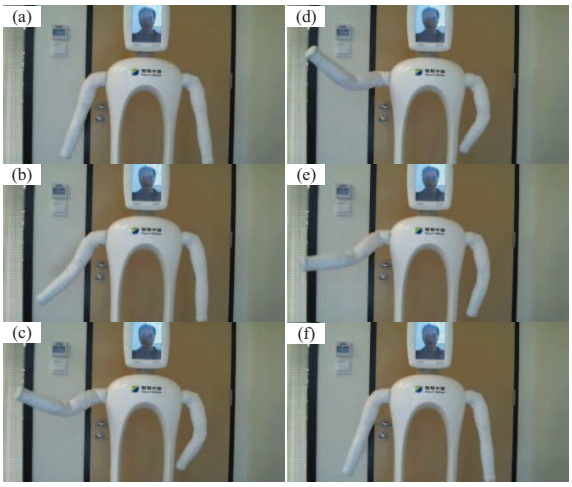

Fig. 15. The robot is dancing with another style

V. CONCLUSIONS AND FUTURE WORK

In conclusion, this paper proposed a novel soft inflatable arm for telepresence robots, and it can imitate human arms to realize remote interaction. The new arm structure is performed by a very common, low cost, and environmental friendly inflatable material, and it is very light, which weight is only about 50 grams, but can well realize agile movement, and the soft inflatable can work just by pumping air with very low pressure (7.32 ± 3.45 kPa), and allows human directly and safely contact without any external sensors. In addition, a new joint model, joint compressed length and joint kinematics are also developed to solve the challenge problems of joint soft inflatable and deformable.

Numerous experiments have been conducted and the results show that the soft inflatable arms not only can agilely move, but also make more complex motions, like dancing. And workspace and velocity are close to an adult's arm movement space and normal motion speed.

In this paper, mechanical design and implementation, joint deformations and kinematics, and some key performances of the soft inflatable arm have been analyzed and evaluated. In the future, more performances of kinematics and dynamics will be evaluated, such as the kinematics of the soft inflatable arm in coordinate system, and these experiments and performances will be implemented and evaluated.

REFERENCES

[1] Antonio Bicchi and Giovanni Toniett, IEEE Robotics and Automation Magazine,June 2004, pp: 22-33.
[2] S. Haddadin, A. Albu-Schaffer, and G. Hirzinger, Safety evaluation of physical human-robot interaction via crash testing, Robot. Sci. Syst. Conf., 2007.
[3] S. Haddadin, A. Albu-Schaffer, and G. Hirzinger, Safe physical human-robot interaction: measurements, analysis and new insights, Int. Symp. Robot. Res., 2007.
[4] M. Zinn, O. Khatib, and B. Roth, A new actuation approach for human friendly robot design, Proc. IEEE Int. Conf. Robotics and Automation, vol. 1, pp. 249-254, 2004.
[5] Keith W. Wait,Philip J. Jackson, and Lanny S. Smoot, Self Locomotion of a Spherical Rolling Robot Using a Novel Deformable Pneumatic Method, 2010 IEEE International Conference on Robotics and Automation Anchorage Convention District May 3-8, 2010, Anchorage, Alaska, USA, pp: 3757-3762.
[6] K. Ikuta, H. Ishii, and M. Nokata, Safety evaluation method of design and control for human-care robots, Int. J. Robot. Res., vol. 22, no. 5, May 2003, pp. 281C297.
[7] H. Kimura, F. Kajimura, D. Maruyama, M. Koseki,N. Inou, Flexible Hermetically-Sealed Mobile Robot for Narrow Spaces Using Hydrostatic Skeleton Driving Mechanism, IEEE/RSJ International Conference on Intelligent Robots and Systems, 2006.J.-C. Thomas, C. Wielgosz, Deflections of highly inflated fabric tubes, Thin-Walled Structures 42(2004), pp: 1049C1066.
[8] N. Salomonski, M. Shoham, G. Grossman, Light Robot Arm Based on Inflatable Structure, Annals of the ClRP Vol. 44/1/1995.
[9] S. Voisembert, A. Riwan, N. Mechbal and A. Barraco, A novel inflatable robot with constant and continuous volume, 2011 IEEE International Conference on Robotics and Automation, May 9-13, 2011, Shanghai, China, pp: 5843-5848.
[10] Yoram Koren, Ann Arbor, Yiechiel Weinstein Misgav, Inflatable structure, US Patent 5065640.
[11] Siddharth Sanan, Soft Robots for Safe Physical Human Interaction, PHD thesis.
[12] R. Baldur and W. Blach, Inflatable manipulator, Society of Manufacturing Engineers, 1985.
[13] S. Voisembert, A. Riwan and N. Mechbal, Numerical Evaluation of a New Robotic Manipulator based on Inflatable Joints., 8th IEEE International Conference on Automation Science and Engineering, August 20-24, 2012, Seoul, Korea, pp: 544-549.
[14] Siddharth Sanan, Justin B. Moidel and Christopher G. Atkeson, Robots with Inflatable Links, The 2009 IEEE/RSJ International Conference on Intelligent Robots and Systems, October 11-15, 2009, St. Louis, USA, pp: 4331-4336.
[15] Siddharth Sanan, Michael H. Ornstein and Christopher G. Atkeson, Physical Human Interaction for an Inflatable Manipulator, 33rd Annual International Conference of the IEEE EMBS Boston, Massachusetts USA, August 30 - September 3, 2011, pp: 7401-7404.
[16] Otherlab, https://otherlab.com/.
[17] Saul Griffith, Otherlab, https://otherlab.com/.
[18] http://hexagon-hg.com.tw/front/bin/ptlist.phtml?Category=712
[19] H. Nagasaki, Asymmetric velocity and acceleration profiles of human arm movements, Exp Brain Res (1989)74, pp: 319-326.
[20] H I Krebs, N Hogan, M L Aisen, B T Volpe, Quantization of Continuous Arm Movements in Humans with Brain Injury, Proc. Nat. Acad. of Science 1999(96), pp: 4645-4649.
[21] B Rohrer, S Fasoli, H I Krebs, R Hughes, B T Volpe, W R Frontera, J Stein, N Hogan, J. Neurosci, Movement Smoothness Changes during Stroke Recovery, 2002(18), pp: 8297-8304.
[22] Submovements Grow Larger, Fewer, and More Blended During Stroke Recovery, B Rohrer, S Fasoli, H I Krebs, B T Volpe, W R Frontera, J Stein, N Hogan, Motor Control, 2004(8), pp: 472-483.
[23] L Dipietro, HI Krebs, B Volpe, N Hogan, Combinations of elementary units underlying human arm movements at different speeds, Society for Neuroscience, Annual Meeting, 2004.
[24] L Dipietro, N Hogan, HI Krebs, B Volpe, Origins of irregularity in human arm movements, Progress in Motor Control V, 2005.